Dimer ordering of CuTtertBuPc molecules on the Ag/Si(111)-$^{(\sqrt{3} \times \sqrt{3})R30°}$ surface: a scanning tunnelling microscopy/spectroscopy study

Dimer ordering of CuTtertBuPc molecules on the Ag/Si(111)-($\sqrt{3} \times \sqrt{3}$)R30° surface: a scanning tunnelling microscopy/spectroscopy study

Sergey A Krasnikov[1,2,5], **Claire J Hanson**[1,3], **Dermot F Brougham**[4] and **Attilio A Cafolla**[1,2]

[1] School of Physical Sciences, Dublin City University, Glasnevin, Dublin 9, Republic of Ireland
[2] Institute for Advanced Material Science (IAMS), Trinity College Dublin, Dublin 2, Republic of Ireland
[3] National Centre for Sensor Research (NCSR), Dublin City University, Glasnevin, Dublin 9, Republic of Ireland
[4] National Institute for Cellular Biotechnology, School of Chemical Sciences, Dublin City University, Glasnevin, Dublin 9, Republic of Ireland

E-mail: Sergey.Krasnikov@dcu.ie

Abstract
The room temperature growth and ordering of copper(II) 2,9,16,23-tetra-*tert*-butyl-phthalocyanine (CuTtertBuPc) molecules on the Ag/Si(111)-($\sqrt{3} \times \sqrt{3}$)R30° surface have been investigated using scanning tunnelling microscopy/spectroscopy (STM/STS). Results indicate a well-ordered molecular layer in which the phthalocyanine molecules have a flat orientation with the molecular plane lying parallel to the substrate and forming a dimer structure on the surface. STS data obtained from one monolayer (ML) of the CuTtertBuPc on the Ag/Si(111)-($\sqrt{3} \times \sqrt{3}$)R30° surface show excellent agreement with valence-band x-ray photoemission and x-ray absorption spectra taken from thin films of CuTtertBuPc (10–20 ML) prepared *in situ* on the clean Si(111) substrate. Combining the spectroscopy results it was found that the highest occupied molecular orbital (HOMO) of the CuTtertBuPc is the half-occupied MO of b_{1g} symmetry with mixed Cu $3d(x^2-y^2)$ and ligand 2p character which was confirmed by density functional theory calculations and x-ray emission spectroscopy data.

1. Introduction

Phthalocyanines represent a class of nearly square planar organic molecules with a two-dimensional conjugated π-electron delocalization [1]. They are among the most important fine chemicals in industry and are utilized in many technological applications such as sensors,

[5] Author to whom any correspondence should be addressed.

organic semiconductors, pigments, dyes, optoelectronic devices, solar cells, catalysis, nonlinear optics and nanomaterials [1, 2]. Furthermore, phthalocyanines are one of the most stable organic materials undergoing no noticeable degradation in air up to about 400 °C. This advantage together with their good ultrahigh vacuum compatibility allows the growth of ultra-clean well-ordered phthalocyanine films of different thickness on various substrates using thermal evaporation. In particular, 3d transition metal (TM) phthalocyanines are widely used in many of the technological applications mentioned above, due to their unique electronic structure, which has been a subject of intense experimental and theoretical research during the last decade [3–19]. The central part of these complexes, including the 3d-atom and its nearest neighbours, is known to be their most reactive component defining the most important applications of these compounds. The occupied and empty 3d electron states of the metal atom, which are located near the Fermi level and are involved in chemical bonding, are essentially responsible for the interesting properties of these 3d compounds. Thus it is evident that a detailed knowledge of the nature of the electronic structure and chemical bonding in these 3d TM macrocyclic rings is required for the realization of their full potential.

In turn, an understanding of the phthalocyanine/inorganic interface is a critical element required for optimizing their use in many of the applications listed above. Organic interfaces with specific electrochemical or photochemical properties are a key technology in realizing new types of organic molecular devices. To establish the actual concept of these devices, it is important to control supramolecular structures on a substrate as well as their function. Of particular interest are the nature of the bonding between the phthalocyanine molecules and the surface, as reflected in the electronic charge distribution, and their geometric configuration at the interface. This information can be obtained by using a combination of scanning tunnelling microscopy (STM) and scanning tunnelling spectroscopy (STS). STM is a highly local technique that has become a powerful tool for studying the adsorption geometry and the conformation and dynamics of single molecules and molecular assemblies on conducting substrates [20–26]. However, while these images elucidate the topographic structure of the interface, they provide little information about its electronic properties. STS, which involves measuring the tunnelling current at fixed tip–surface separation as the bias voltage is systematically varied ($I(V)$ spectroscopy), is perhaps one of the best tools for probing local electronic structure with molecular spatial resolution. STS is unique in that it allows both the filled and empty state density at the surface to be probed in a single measurement providing local density of states information close to the Fermi level.

The present work is aimed at investigating the molecular assembly of copper(II) 2,9,16,23-tetra-*tert*-butyl-phthalocyanine (CuTtertBuPc) on the Ag/Si(111)-($\sqrt{3} \times \sqrt{3}$)R30° surface in order to reveal the conformational behaviour of CuTtertBuPc molecules in the submonolayer to monolayer regime by using STM. In turn, STS is utilized to obtain information about the local density of states. A comparison of STS results with x-ray spectroscopic data provides a complete picture of the occupied and unoccupied density of states near the Fermi level. The results of this work yield important information about the electronic and structural properties of these phthalocyanine molecules adsorbed on the Ag/Si(111)-($\sqrt{3} \times \sqrt{3}$)R30° surface.

2. Experimental details

The STM/STS experiments were performed at room temperature (RT), using a commercial instrument (Omicron Vakumphysik GmbH), in an ultra-high-vacuum (UHV) system consisting of an analysis chamber (with a base pressure of 2×10^{-11} mbar) and a preparation chamber (5×10^{-11} mbar). An electrochemically etched polycrystalline Pt/Ir tip was used. STM images were recorded in constant current mode. The voltage V_{sample} corresponds to the sample bias

with respect to the tip. No smoothing or drift corrections have been applied to any of the STM images presented in this paper. The Si(111) substrate was p-type boron-doped with a resistivity in the range 0.1–1.0 Ω cm. Atomically clean Si(111)-(7 $\times$ 7) surfaces were prepared in the usual manner by *in situ* direct current heating to 1520 K after the samples were first degassed at 870 K for 12 h. The clean Si(111)-(7 $\times$ 7) surface was checked by low-energy electron diffraction (LEED) and STM before preparation of the Ag/Si(111)-($\sqrt{3} \times \sqrt{3}$)R30° surface. Silver (Goodfellow Metals, 5 N) was deposited by e-beam evaporation from a molybdenum crucible onto the Si substrate, which was maintained at 770 K during the deposition. The cleanliness of the Ag/Si(111)-($\sqrt{3} \times \sqrt{3}$)R30° surface was verified by STM and LEED before phthalocyanine deposition. CuTtertBuPc (Aldrich Chemicals) was evaporated in a preparation chamber isolated from the STM chamber at a rate of about 0.2 ML (monolayer) per minute from a tantalum crucible in a homemade deposition cell operated at a temperature of approximately 600 K. The total pressure during phthalocyanine deposition was in the 10^{-9} mbar range. Before evaporation the phthalocyanine powder was degassed for about 12 h to remove water vapour.

Tunnelling spectra were acquired on a grid of specified points within an image. At each grid point the scan is interrupted during imaging; the feedback loop is switched off and, after a short delay time to allow stabilization of the current preamplifier, a voltage ramp is applied. In between the grid points the feedback is on and the STM operates in constant current mode. While recording $I(V)$ spectra it was ensured that current measurements did not exceed the dynamic range of the current preamplifier. Before and after $I(V)$ spectra acquisition the quality of the surface was verified by STM imaging to ensure that no damage was done to the measured layer.

The x-ray photoemission spectroscopy (XPS) measurements on CuTtertBuPc were performed at the beamline 4.1 at the SRS storage ring (Daresbury, UK) using a surface science end station (with a base pressure of 1×10^{-10} mbar) equipped with a Scienta SES200 hemispherical electron energy analyser with an acceptance angle of $\pm 3°$. The total energy resolution was about 100 meV for the x-ray photoemission spectra taken at excitation photon energies in the range 60–130 eV. The sample was a thin film of CuTtertBuPc (10–20 ML) evaporated *in situ* onto a clean Si(111) substrate using the procedure described above. The x-ray absorption spectroscopy (XAS) measurements were performed at the Russian–German beamline at the BESSY II storage ring (Berlin, Germany) and the SX-700 beamline at the ASTRID storage ring (Aarhus, Denmark). The estimated photon-energy resolution at the Cu 2p ($\sim$930 eV), N 1s ($\sim$400 eV) and C 1s ($\sim$290 eV) absorption thresholds was better than 200 meV, 100 meV and 80 meV, respectively. The spectra were normalized to the incident photon flux monitored by a gold grid.

3. Results and discussion

Silver deposition on the Si(111)-(7 $\times$ 7) surface at elevated temperatures forms a ($\sqrt{3} \times \sqrt{3}$)R30° reconstruction [25–28]. At room temperature the clean Ag/Si(111)-($\sqrt{3} \times \sqrt{3}$)R30° surface is well described by the honeycomb–chain–trimer model. Figure 1 shows a typical STM occupied state image of this surface recorded at sample bias $V_{sample} = -1.0$ V. This STM image reveals hexagonal features consisting of six protrusions (honeycomb structure), relating to the charge density at the centre of the Ag trimers, while the dark regions are associated with the Si trimers. The average length of the unit cell is measured to be 0.68 ± 0.05 nm. This clean Ag/Si(111)-($\sqrt{3} \times \sqrt{3}$)R30° surface was used as the substrate for the preparation of ultrathin CuTtertBuPc layers.

Figure 2 shows typical STM images taken from approximately 1 ML of the CuTtertBuPc on the Ag/Si(111)-($\sqrt{3} \times \sqrt{3}$)R30° surface. CuTtertBuPc deposits on the surface, forming
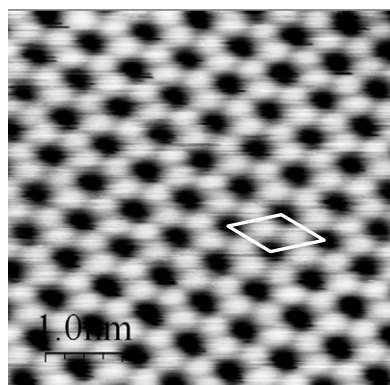
Figure 1. STM image of the hexagonal–chain–trimer structure of the silver passivated Si(111) surface. The $\sqrt{3} \times \sqrt{3}$ unit cell is marked in white. Image parameters are $V_{sample} = -1.0$ V, $I_t = 0.2$ nA, size = 5 nm $\times$ 5 nm.

rows of molecules as can be clearly seen in figure 2. Each molecule has a flat orientation on the surface with molecular planes lying parallel to the substrate. The rows are made up of groups of two molecules aligned together (dimers). The rows have a well-organized structure and grow in lines parallel to each other. The STM image obtained using a positive (negative) sample bias shows empty states (filled states) of the molecule as electrons are tunnelling from the tip to the sample (sample to the tip). Figure 2 gives an example of images taken with a negative sample bias (a), (c) and with a positive sample bias (b), (d). In figure 2(a), representing filled states, the dimers of the CuTtertBuPc molecules can be seen as a pairs of bright protrusions with each showing a four-fold symmetry. In figure 2(b) the *tert*-butyl groups can be seen as bright dots, where each *tert*-butyl group contributes to the rhomboid shaped features consisting of four such groups, while the phthalocyanine rings are imaged as dark circles. The unit cell of the CuTtertBuPc lattice (shown in white in figure 2(a) or in black in figure 2(b)) contains two phthalocyanine molecules forming a dimer and has the following dimensions: 3.10 ± 0.03 nm by 1.85 ± 0.02 nm, with a ratio of 1.68, while the angle between the unit cell vectors is $86° \pm 1°$, thus the structure has an oblique lattice. In figure 2(c) two large domains of the CuTtertBuPc molecules possessing an ordered dimer structure are seen. These domains are separated by three parallel rows of single phthalocyanine molecules indicated by arrows on the image. The distance between these molecular rows is slightly bigger than that between the rows forming a dimer structure. Disordered molecules can be seen at the step edge of a silver terrace (left top corner of figure 2(c)).

Figure 2(d) shows another example of a domain boundary that consists of several parallel rows of CuTtertBuPc molecules. In each of these rows some of the individual phthalocyanine molecules have a random orientation leading to some degree of disorder. The lower domain, possessing an ordered dimer structure, has several defects (missing phthalocyanine molecules) marked by circles on the image 2(d).

Previous STM observations of copper phthalocyanine molecules on different substrates show a complex behaviour and ordering of the molecules, which depends on the substrate reactivity, substrate temperature and the nature of the outer substituents attached to the CuPc macrocycle [21–24, 29, 30]. On passive substrates, such as highly oriented pyrolytic graphite (HOPG), hydrogen passivated silicon and gold, the unsubstituted CuPc molecules form an oblique structure [23, 24, 29, 30] or elongated molecular-like nanolines [22]. Depending on the nature of the outer substituents (their length and attachment position to the macrocycle)
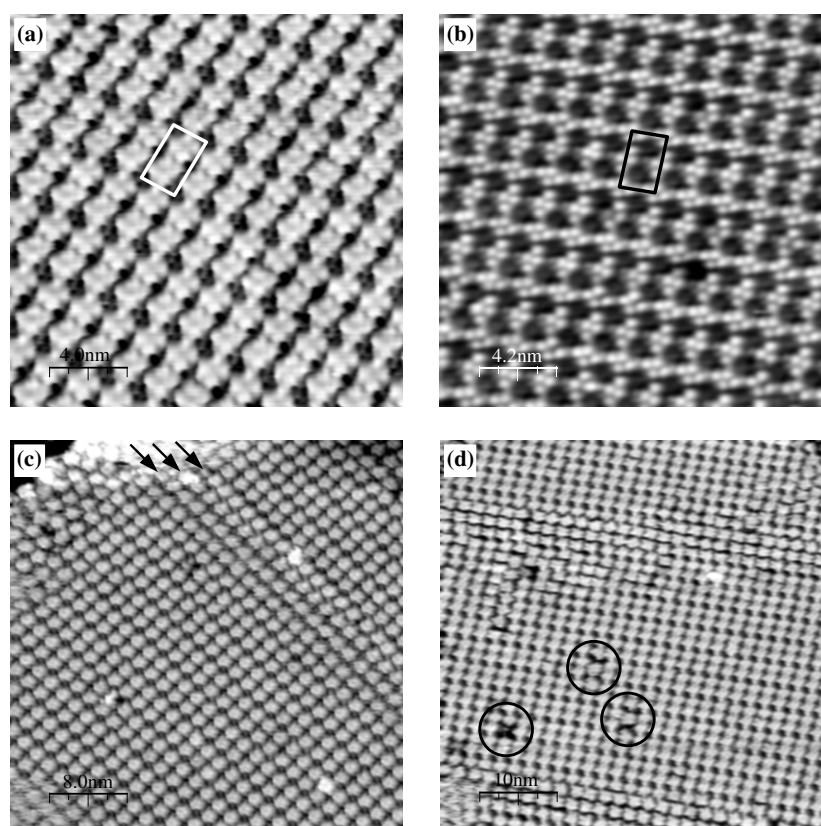
Figure 2. STM images of CuTtertBuPc molecules on the Ag/Si(111)-($\sqrt{3} \times \sqrt{3}$)R30° surface. Image parameters are: (a) $V_{sample} = -1.75$ V, $I_t = 0.9$ nA, size = 20 nm × 20 nm; (b) $V_{sample} = +1.25$ V, $I_t = 0.25$ nA, size = 21 nm × 21 nm; (c) $V_{sample} = -1.75$ V, $I_t = 1.0$ nA, size = 40 nm × 40 nm; (d) $V_{sample} = +2.0$ V, $I_t = 0.75$ nA, size = 50 nm × 50 nm. The unit cell is shown in white (a) and black (b). The unit cell vectors, **a** and **b**, are 3.10 nm and 1.85 nm, respectively, with an angle of 86° between them. Arrows indicate boundary rows between two domains of dimers. Circles indicate missing CuTtertBuPc molecules.

close-packed domains containing parallel rows of modified copper phthalocyanine molecules [23], hexagonal [23] and oblique [23, 24] structures were observed. In the case of the CuTtertBuPc molecules adsorbed on the Ag/Si(111)-($\sqrt{3} \times \sqrt{3}$)R30° surface *tert*-butyl groups attached to the benzyl rings of the phthalocyanine macrocycle play a significant role in forming the observed dimer structure. On a low-reactivity substrate such as Ag passivated Si the deposited CuTtertBuPc molecules are quite mobile. This makes room temperature STM imaging of the molecules difficult at low surface coverage, because individual molecules can be easily dragged by the STM tip. Such mobility on the surface favours the formation of a close packed layer. In this close packed layer the *tert*-butyl groups prefer to form the observed rhomboid shaped features defining the position of each molecule and leading to a dimer structure.

The CuTtertBuPc molecules form large (approximately 40 nm × 40 nm) domains of dimers on the Ag/Si(111)-($\sqrt{3} \times \sqrt{3}$)R30° surface when the thickness of the phthalocyanine layer is close to 1 ML. An example of such long range order is shown in figure 3(a). The inset in figure 3(a) shows a proposed model for the adsorption sites of the molecules on the surface.
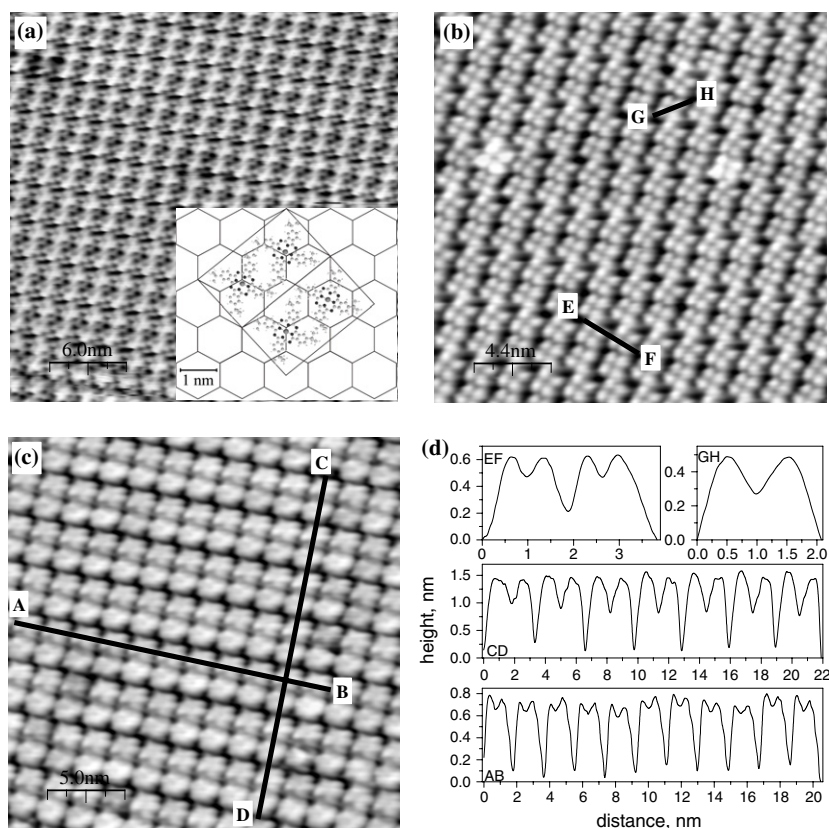
Figure 3. STM images of CuTtertBuPc molecules on the Ag/Si(111)-($\sqrt{3} \times \sqrt{3}$)R30° surface. Image parameters are: (a) $V_{sample} = +2.0$ V, $I_t = 0.5$ nA, size = 30 nm × 30 nm; (b) $V_{sample} = -2.0$ V, $I_t = 0.25$ nA, size = 22 nm × 22 nm; (c) $V_{sample} = -1.75$ V, $I_t = 1.0$ nA, size = 25 nm × 25 nm. (d) Corresponding height profiles indicated by lines on the images (b) and (c). The inset in (a) shows a proposed model for the adsorption sites of the molecules on the Ag/Si(111) surface.

Figure 3(b) shows two CuTtertBuPc molecules lying on top of first phthalocyanine monolayer. It is easy to see that the second layer molecules are covering the first layer CuTtertBuPc molecules, preserving the same orientation. The four-fold symmetry of the each CuTtertBuPc molecule is clearly seen from figure 3(b). Figure 3(d) shows height profiles taken from domains of well-ordered CuTtertBuPc dimers from which the size of the individual molecule can be roughly estimated. The AB and CD height profiles confirm the unit cell parameters to be 3.1 by 1.85 nm and show quite a uniform height distribution along these directions. The GH profile shows the diagonal size of the phthalocyanine macrocycle (without the *tert*-butyl groups) to be approximately 2.1 nm.

Figure 4 shows $I(V)$ spectra recorded during STM image acquisition from 1 ML of the CuTtertBuPc on the Ag/Si(111)-($\sqrt{3} \times \sqrt{3}$)R30° surface (a) and the corresponding normalized conductivity spectra $(dI/dV)/(I/V)$ which are proportional to the density of states (b). The normalized conductivity spectra were obtained by numerical differentiation of the $I(V)$ spectra shown in figure 4(a). Each spectrum is the result of averaging over 2500 spectra taken within an image using a grid of specified points. The spectra 1, 3 and 4 were recorded over the area of the image shown in figure 3(c) using the same sample bias but different initial tunnelling
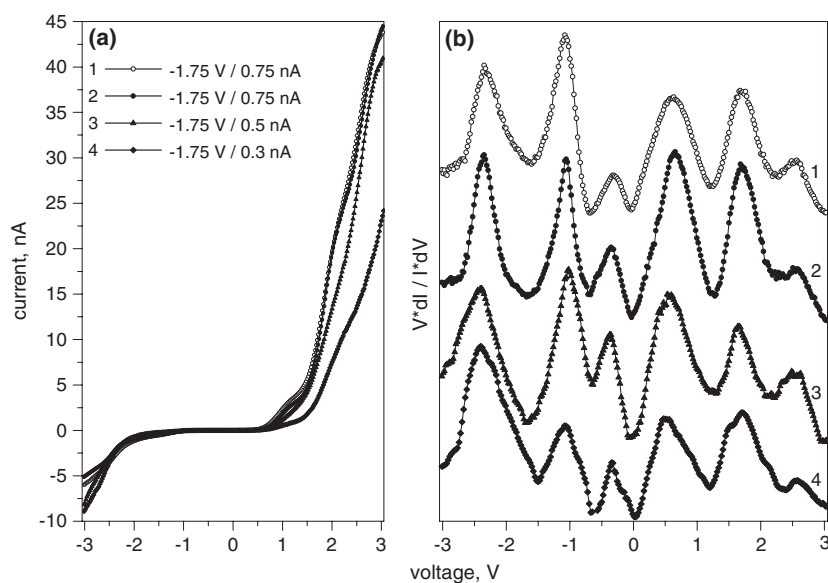
Figure 4. $I(V)$ spectra recorded during STM image acquisition from 1 ML of CuTtertBuPc on the Ag/Si(111)-($\sqrt{3} \times \sqrt{3}$)R30° surface (a) and corresponding normalized conductivity spectra $(\mathrm{d}I/\mathrm{d}V)/(I/V)$ representing the density of states (b). The spectra 1, 3 and 4 were averaged over 2500 points in the area of the image shown in figure 3(c). Spectrum 2 was acquired from a different area of the sample and averaged over the same number of points.

current settings. These different initial settings correspond to different tip-to-sample distances during acquisition of the $I(V)$ spectrum. Spectrum 2 was acquired from a different area of the sample. The results show excellent reproducibility and agreement between the spectra obtained. Each spectrum shows six prominent features: three peaks observed at −2.3, −1.1 and −0.4 V are related to occupied states and three peaks observed at 0.7, 1.7 and 2.6 V to unoccupied states. STS measurements repeated on different areas of the CuTtertBuPc layer show that these features are reproducible. The assignment of these peaks is discussed below when comparing the STS spectra with valence band XPS, XAS and theoretical calculation results.

Figure 5 shows normalized conductivity spectra taken from the ordered CuTtertBuPc layer (spectra 1 and 2) and from the clean Ag/Si(111)-($\sqrt{3} \times \sqrt{3}$)R30° surface (spectra 3 and 4). For comparison the valence band XPS spectrum measured from a clean Ag(100) single crystal [31] is shown by the solid line (spectrum 5). From figure 5 it is seen that there is no significant contribution of the substrate signal to STS spectra measured from the CuTtertBuPc layer. Characteristic features of the substrate spectrum occur at energies corresponding to signal minima in the STS spectrum obtained from the phthalocyanine layer. Only the peak at 1.7 V, related to an empty state, is present in both the CuTtertBuPc layer and substrate spectra. However, in the case of the clean Ag/Si(111)-($\sqrt{3} \times \sqrt{3}$)R30° surface this peak has two additional shoulders, which are absent in the STS spectra of the CuTtertBuPc layer. These facts allow us to conclude that no spectral features related to a signal from the substrate are present in the STS spectra measured from the ordered phthalocyanine layer.

In order to assign peaks obtained in STS spectra a comparison with results measured using other spectroscopic techniques and theoretical calculations is required. Figure 6 shows an STS spectrum of the ordered CuTtertBuPc layer on the Ag/Si(111)-($\sqrt{3} \times \sqrt{3}$)R30° surface compared to a valence band (VB) XPS spectrum acquired at normal emission using an
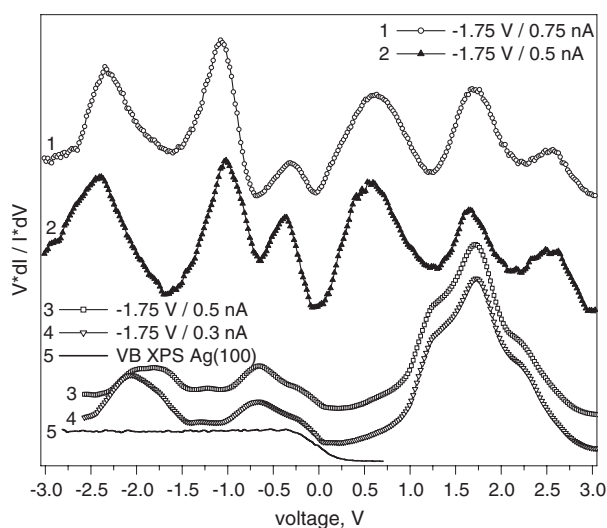
Figure 5. Comparison between normalized conductivity spectra obtained from the CuTtertBuPc layer (1 and 2) and from the clean Ag/Si(111)-($\sqrt{3} \times \sqrt{3}$)R30° surface (3 and 4). The solid line shows a valence band XPS spectrum taken from a Ag(100) single crystal.
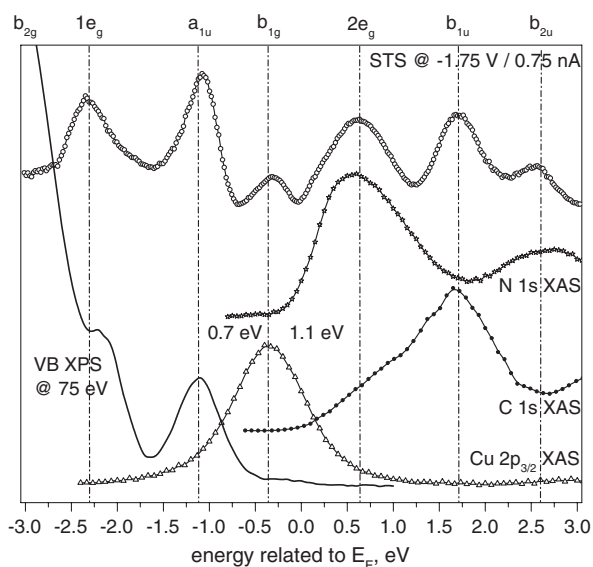

Figure 6. Comparison between the normalized conductivity spectrum measured from 1 ML of the CuTtertBuPc on the Ag/Si(111)-($\sqrt{3} \times \sqrt{3}$)R30° surface and the valence band XPS, C 1s, N 1s, Cu 2p$_{3/2}$ XAS spectra measured from thin films of CuTtertBuPc (10–20 ML) prepared *in situ* on a clean Si(111) substrate. The energy scales of the absorption spectra are aligned using the core level energies, E (C 1s) = 284.45 eV, E (N 1s) = 398.5 eV and E(Cu 2p$_{3/2}$) = 934.5 eV.

excitation photon energy of 75 eV and to the C 1s, N 1s and Cu 2p$_{3/2}$ XAS spectra measured from thin films of the CuTtertBuPc (10–20 ML) prepared *in situ* on the clean Si(111) substrate. The energy scales of the absorption spectra are aligned using the core level energies, E (C 1s) = 284.45 eV, E (N 1s) = 398.5 eV and E (Cu 2p$_{3/2}$) = 934.5 eV, measured in the present

study which agree well with core level XPS results known in literature [6, 14, 15, 32]. A good correlation between the spectra is clearly seen. The following peak assignment can be made by comparing these results with electronic structure calculations using density functional theory [4, 11]. The peak observed at -0.4 eV corresponds to the highest occupied molecular orbital (HOMO) having b_{1g} symmetry. The HOMO is a half-occupied σ-molecular orbital (MO) and has mixed Cu $3d(x^2-y^2)$ and ligand $2p$ character [4]. The copper atom in copper phthalocyanine formally has the electron configuration of the Cu^{2+} ion ([Ar] $3d^9$) with one missing $3d$ electron. The main peak in the Cu $2p_{3/2}$ x-ray absorption spectrum results from the dipole-allowed transition of the $2p_{3/2}$ electron to this empty $3d$ state. The energy position of the Cu $2p_{3/2}$ XAS peak correlates well with the energy position of the first STS peak (at -0.4 V) related to occupied states. This fact confirms that the HOMO is half-occupied and has mainly Cu $3d$ character. The next two occupied states, at -2.3 and -1.1 eV, are molecular orbitals having e_g and a_{1u} symmetry, respectively. The a_{1u} π-MO mainly consists of C $2p$ states [4, 5]. The unoccupied states situated at 0.7, 1.7 and 2.6 eV correspond to MOs of e_g, b_{1u} and b_{2u} symmetry, respectively. The $2e_g$ π-MO is the lowest unoccupied molecular orbital (LUMO). Comparing the STS data with the XAS spectra it is seen that the $2e_g$ and b_{2u} MOs have a mixed ligand $2p$ character. In turn, the b_{1u} MO comprises mostly empty C $2p$ states.

Using a complete density of states picture obtained from STS, VB XPS and XAS data analysis the band gap in CuTtertBuPc can be estimated. The optical band gap in CuPc defined by the optically allowed transition $a_{1u}(\pi)$–$e_g(\pi^*)$ is known to be 1.7–1.75 eV [33–35] which is in good agreement with the a_{1u}–$2e_g$ energy separation (1.8 eV) obtained from STS spectra of CuTtertBuPc. In turn, a HOMO–LUMO (b_{1g}–$2e_g$) band gap obtained from STS spectra is equal to 1.1 eV, which corresponds to a transport band gap in CuTtertBuPc. This value is in excellent agreement with $z(V)$ spectroscopy results performed on CuPc thin films using STM [29] and density functional theory calculations [4, 11]. Furthermore, two discrete occupied states (a_{1u} and b_{1g}) separated by 0.8 eV and located near the Fermi level were observed during x-ray emission measurements performed on 200 nm thick CuPc films prepared on the P:Si(100) substrate [3, 17]. In these experiments the energy position of the a_{1u} peak was found to agree well with UPS data in the literature [8–10, 12, 14–16, 36], which, in turn, have excellent agreement with STS and VB XPS spectra obtained in this work. The peak related to the b_{1g} MO is barely visible in CuPc UPS and VB XPS spectra reported in the literature. It can be related to the ionization character of these spectroscopic techniques leading to strong final state effects, which could modify the binding energy of the b_{1g} state. In this case photoemission from the a_{1u} and b_{1g} states can overlap in energy, resulting in a broad asymmetric feature which can be observed only in high-resolution measurements [12]. In the case of STS there is no influence of the final state effect, since the kinetic energy of the outgoing (or incoming) electrons recorded in the photoemission experiment is irrelevant for this type of measurement. Only the total number of such electrons contributing to the magnitude of the tunnelling current is relevant.

In conclusion, the room temperature growth and ordering of the CuTtertBuPc on the Ag/Si(111)-($\sqrt{3} \times \sqrt{3}$)R30° surface have been investigated using scanning tunnelling microscopy and spectroscopy. A well-ordered molecular layer was obtained in which the phthalocyanine molecules have a flat orientation with molecular planes lying parallel to the surface and form a dimer structure. STS data obtained from one monolayer of CuTtertBuPc on the Ag/Si(111)-($\sqrt{3} \times \sqrt{3}$)R30° surface show excellent agreement with valence band x-ray photoemission and x-ray absorption spectra taken from thin films of the CuTtertBuPc (10–20 ML) prepared *in situ* on a clean Si(111) substrate, as well as with x-ray emission spectroscopy data, optical band gap measurements and density functional theory calculations. The HOMO in the CuTtertBuPc is the half-occupied σ-MO of b_{1g} symmetry with mixed Cu $3d(x^2-y^2)$ and ligand $2p$ character. The LUMO is π-MO of e_g symmetry with mainly ligand

(C and N) 2p character. Scanning tunnelling spectroscopy has been shown to be a prospective tool for probing the local electronic structure and providing complete density of states information close to the Fermi level.

Acknowledgments

References

[1] Leznoff C C and Lever A B P (ed) 1993 *Phthalocyanines, Properties and Applications* vol 3 (New York: VCH Publishers)
[2] Simon J and André J-J 1985 *Molecular Semiconductors* (Berlin: Springer)
[3] Downes J E, McGuinness C, Glans P-A, Learmonth T, Fu D, Sheridan P and Smith K E 2004 *Chem. Phys. Lett.* **390** 203
[4] Liao M-S and Scheiner S 2001 *J. Chem. Phys.* **114** 9780
[5] Kurmaev E Z, Shamin S N, Galakhov V R, Moewes A, Otsuka T, Koizume S, Endo K, Katz H E, Bach M, Neumann M, Ederer D L and Iwami M 2001 *Phys. Rev.* B **64** 045211
[6] Dufour G, Poncey C, Rochet F, Roulet H, Sacchi M, De Santis M and De Crescenzi M 1994 *Surf. Sci.* **319** 251
[7] Dufour G, Poncey C, Rochet F, Roulet H, Iacobucci S, Sacchi M, Yubero F, Motta N, Piancastelli M N, Sgarlata A and De Crescenzi M 1995 *J. Electron Spectrosc. Relat. Phenom.* **76** 219
[8] Ellis T S, Park K T, Hulbert S L, Ulrich M D and Rowe J E 2004 *J. Appl. Phys.* **95** 982
[9] Gorgoi M and Zahn D R T 2006 *Appl. Surf. Sci.* **252** 5453
[10] Hill I G, Kahn A, Soos Z G and Pascal R A Jr 2000 *Chem. Phys. Lett.* **327** 181
[11] Rosa A and Baerends E J 1994 *Inorg. Chem.* **33** 584
[12] Kera S, Yamane H, Sakuragi I, Okudaira K K and Ueno N 2002 *Chem. Phys. Lett.* **364** 93
[13] Lozzi L, Santucci S, La Rosa S, Delley B and Picozzi S 2004 *J. Chem. Phys.* **121** 1883
[14] Schwieger T, Peisert H, Golden M S, Knupfer M and Fink J 2002 *Phys. Rev.* B **66** 155207
[15] Peisert H, Knupfer M, Schwieger T, Auerhammer J M, Golden M S and Fink J 2002 *J. Appl. Phys.* **91** 4872
[16] Peisert H, Knupfer M and Fink J 2002 *Surf. Sci.* **515** 491
[17] Zhang Y, Downes J E, Wang S, Learmonth T, Plucinski L, Matsuura A Y, McGuinness C, Glans P-A, Bernardis S, O'Donnell C and Smith K E 2006 *Thin Solid Films* **515** 394
[18] Krasnikov S A, Preobrajenski A B, Sergeeva N N, Brzhezinskaya M M, Nesterov M A, Cafolla A A, Senge M O and Vinogradov A S 2007 *Chem. Phys.* **332** 318
[19] Aristov V Yu, Molodtsova O V, Zhilin V M, Vyalikh D V and Knupfer M 2005 *Phys. Rev.* B **72** 165318
[20] Grütter P, Hofer W and Rosei F (ed) 2006 *Properties of Single Organic Molecules on Crystal Surfaces* (London: Imperial College Press)
[21] Lippel P H, Wilson R J, Miller M D, Wöll Ch and Chiang S 1989 *Phys. Rev. Lett.* **62** 171
[22] Suzuki Y, Hietschold M and Zahn D R T 2006 *Appl. Surf. Sci.* **252** 5449
[23] Lei S-B, Wang C, Wan L-J and Bai C-L 2003 *Japan. J. Appl. Phys.* **42** 4729
[24] Qiu X, Wang C, Zeng Q, Xu B, Yin S, Wang H, Xu S and Bai C 2000 *J. Am. Chem. Soc.* **122** 5550
[25] Guaino Ph, Cafolla A A, Carty D, Sheerin G and Hughes G 2003 *Surf. Sci.* **540** 107
[26] Sheerin G and Cafolla A A 2005 *Surf. Sci.* **577** 211
[27] Wilson R J and Chiang S 1987 *Phys. Rev. Lett.* **58** 369
[28] van Loenen E J, Demuth J E, Tromp R M and Hamers R J 1987 *Phys. Rev. Lett.* **58** 373
[29] Alvarado S F, Rossi L, Müller P and Rieß W 2001 *Synth. Met.* **122** 73
[30] Lu X, Hipps K W, Wang X D and Mazur U 1996 *J. Am. Chem. Soc.* **118** 7197
[31] Krasnikov S A, Preobrajenski A B, Chassé T and Szargan R 2003 *Thin Solid Films* **428** 201
[32] Park K T, Miller A, Klier K, Opila R L and Rowe J E 2003 *Surf. Sci.* **529** L285
[33] Lucia E A and Verderame F D 1968 *J. Chem. Phys.* **48** 2674
[34] Schechtman B H and Spicer W E 1970 *J. Mol. Spectrosc.* **33** 28
[35] Yoshida H, Tokura Y and Koda T 1986 *Chem. Phys.* **109** 375
[36] Chassé T, Wu C-I, Hill I G and Kahn A 1999 *J. Appl. Phys.* **85** 6589